ChemPubSoc Europe

DOI: 10.1002/chem.201304779

CHEMISTRY
A European Journal
Communication

Host–Guest Systems

Trapping of Organophosphorus Chemical Nerve Agents in Water with Amino Acid Functionalized Baskets

Yian Ruan,[a] Erdin Dalkiliç,[b] Paul W. Peterson,[a] Aroh Pandit,[a] Arif Dastan,[b] Jason D. Brown,[a] Shane M. Polen,[a] Christopher M. Hadad,[a] and Jovica D. Badjić*[a]

Abstract: We prepared eleven amino-acid functionalized baskets and used ^{1}H NMR spectroscopy to quantify their affinity for entrapping dimethyl methylphosphonate (DMMP, 118 Å^3) in aqueous phosphate buffer at pH = 7.0 ± 0.1; note that DMMP guest is akin in size to chemical nerve agent sarin (132 Å^3). The binding interaction (K_a) was found to vary with the size of substituent groups at the basket's rim. In particular, the degree of branching at the first carbon of each substituent had the greatest effect on the host-guest interaction, as described with the Verloop's B1 steric parameter. The branching at the remote carbons, however, did not perturb the encapsulation, which is important for guiding the design of more effective hosts and catalysts in future.

A paucity of chemoreceptors capable of recognizing organophosphorus (OP) chemical nerve agents[1] contribute to difficulties related to developing effective sensors, degradation catalysts and/or sequestration agents.[2] In particular, recent developments in Syria attest to the challenges pertaining to the identification of sarin and its by-products in the environment, following acts of chemical warfare.[3] Notably, chemical nerve agents have a sufficiently long lifetime in water[4] to act as potent inhibitors of acetylcholinesterase (AChE), causing the accumulation of acetylcholine in neuromuscular junctions and therefore overstimulation of muscles, which in severe cases results in asphyxiation and death.[5] Butyrylcholinesterase (BuChE)[6] and paraoxonase-1 (PON1)[7] enzymes are bioscavengers of OP nerve agents and could remove these toxic compounds from the bloodstream, thereby constituting potential prophylactic, as well as post-exposure, therapeutic measures.[3] As an alternative to these particular therapies, which require significant quantities of enzymes, one can envision that the isolation of OP nerve agents in the interior of concave artificial hosts[1h] might engender a useful strategy for removing undesired OP compounds from the environment. In particular, the advent of supramolecular encapsulation chemistry[8] has led to the understanding that the formation of "molecule within molecule" complexes[9] (k_{in}) is a rapid process, which could be controlled by gating.[10] However, the dissipation of encapsulation complexes is slower with the rate coefficient k_{off} often corresponding to the thermodynamic stability K_a.[11] Accordingly, we reason that preparing artificial hosts complementary to OP nerve agents could be important for 1) creating practical and catalytic alternatives to BuChE/PON1; and 2) obtaining new supramolecular sensors[12] and/or degradation catalysts.[13] We hereby describe an important step toward reaching such an objective: a series of baskets of type **1**–**7** were found to trap dimethyl methylphosphonate (DMMP, 118 Å^3), akin in size to sarin (132 Å^3), and in water (Figure 1). The guest populates the hydrophobic interior of these concave hosts while interacting with amino acid residues at the rim.

Symmetric baskets C_3 of type **1**–**7** were designed to carry three negatively charged carboxylates (pH 7.0) at the rim for enhancing their solubility in water (Figure 1 A and B). The question to be answered is whether these cavitands, comprising two nonpolar regions and a polar belt aggregate in water (Figure 1 B)[14] will bind to small organophosphonates in the manner akin to previously studied baskets?[14–15]

Cavitands **1**–**7** were prepared by the conjugation of tris(anhydride) **8** and hydrophobic amino acids in DMSO at 120 °C (yield 32–57 %). Upon chromatographic purification, each of the baskets was dissolved in $CDCl_3/CD_3OH$ (9:1) and then deprotonated with $(CH_3)_4NOH$ to give the corresponding carboxylate salts. Subsequently, each tetramethylammonium compound (0.1–5.0 mM) was solubilized in aqueous phosphate buffer (pH 7.0 ± 0.1) and then used in our experiments.

^{1}H NMR spectra of [**1**–**7**]$^{3-}$ revealed a set of signals corresponding to C_3 or, perhaps, even more symmetric species (Figure 2; see also Figures S1–S5 in the Supporting Information). In particular, the resonance frequency of proton nuclei, comprising amino acid residues, were found upfield in [**1**-**7**]$^{3-}$ with respect to the analogous signals corresponding to model compounds [**9**–**15**]$^{1-}$ (Figure 2); note that the magnetic shielding was particularly manifested in the case of phenylalanine basket [**7**]$^{3-}$ (Figure 2 B). Although the model compounds are symmetric about the flat phthalimide ring, baskets [**1**–**7**]$^{3-}$ possess two distinct environments that we hereby refer to as their inner and outer sides (Figure 1 B and Table 1). With this designation, our NMR results suggest that aliphatic/aromatic side

[a] Y. Ruan, P. W. Peterson, A. Pandit, J. D. Brown, S. M. Polen, Prof. C. M. Hadad, Prof. J. D. Badjić
Department of Chemistry and Biochemistry, The Ohio State University
100 West 18th Avenue, Columbus OH 43210 (USA)
Fax: (+1) 614-292-1685
E-mail: badjic@chemistry.ohio-state.edu

[b] E. Dalkiliç, Prof. A. Dastan
Department of Chemistry, Ataturk University, Faculty of Sciences
25240 Erzurum (Turkey)

Supporting information for this article is available on the WWW under http://dx.doi.org/10.1002/chem.201304779.

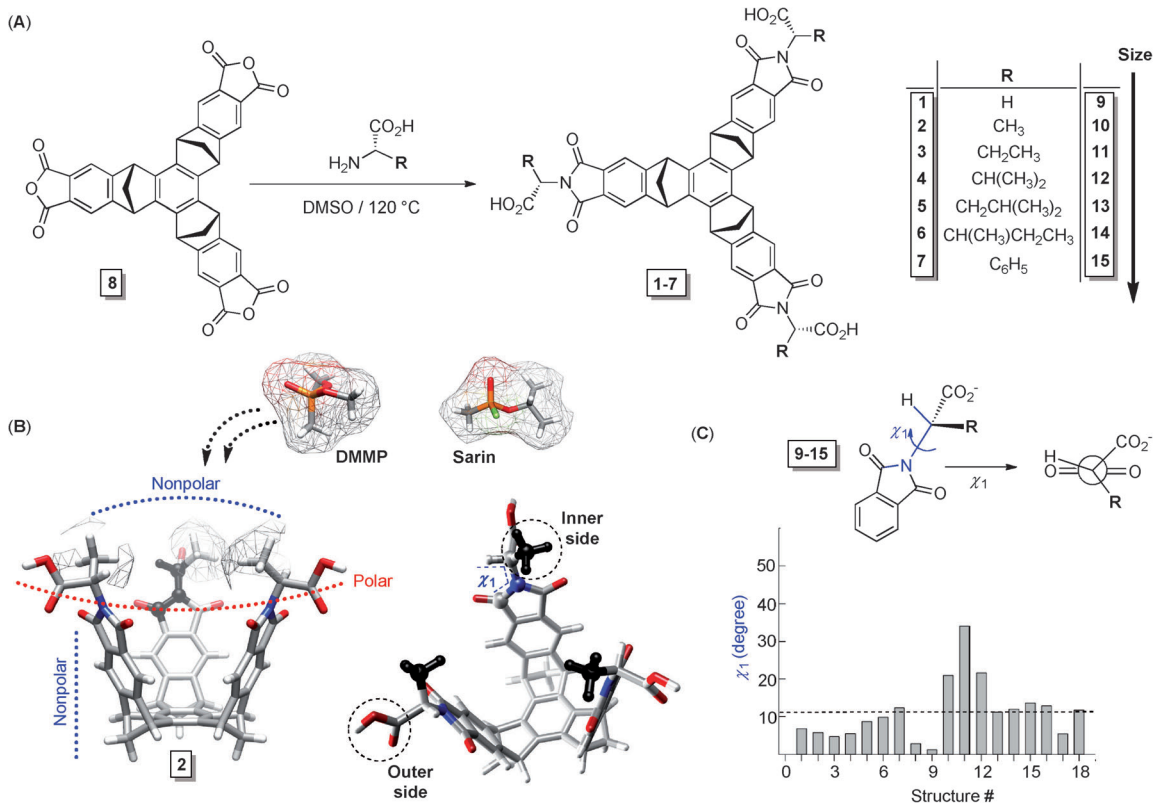

Figure 1. A) Baskets **1**–**7** were prepared by the condensation of tris(anhydride) **8** and hydrophobic amino acids having increasingly bigger functional groups. B) Energy-minimized (MMFFs, Spartan) structure of basket **2** containing (*S*)-alanine at the rim. C) The inspection of solid-state structures of 18 amino acid conjugates of phthalimide (CSD) reveals a conformational bias about the χ_1 torsion with a disposition toward $\chi_1 = 11.1 \pm 7.9^\circ$.

Table 1. Diffusion coefficients (*D*) for baskets (1.0 mM) obtained from DOSY NMR spectroscopic measurements at 298.1 K.

Basket	D [10^{-10} $m^2 s^{-1}$]	r_H [Å][a]	r [Å][b]	r_H [Å][c]
$[\mathbf{1}]^{3-}$	3.3 ± 1.0	7.4 ± 1.8	7	6.6 ± 0.3
$[\mathbf{2}]^{3-}$	3.4 ± 1.0	7.2 ± 1.6	7	6.0 ± 0.4
$[\mathbf{4}]^{3-}$	2.9 ± 1.1	8.3 ± 2.2	7	8.6 ± 2.2
$[\mathbf{7}]^{3-}$	3.0 ± 1.1	8.2 ± 2.1	8	–

[a] Hydrodynamic radius. [b] Computed radius; MMFFs (Spartan). [c] With a large excess of DMMP guest. The hydrodynamic radii were computed by using the Stokes–Einstein equation; the viscosity of 10.0 mM phosphate buffer at pH 7.0 ± 0.1 is similar to that of pure water ($\eta =$ 0.89 MPa s at 25.0 °C).

chains in $[\mathbf{1}\text{–}\mathbf{7}]^{3-}$ reside at the basket inner side, that is, in the vicinity of the concave hydrophobic cavity. In this way, the aromatic rings comprising the cavity of baskets alter the magnetic environment of juxtaposed proton nuclei to, by diamagnetic shielding, reduce their chemical shift (Figure 2). While the hydrophobic side chains point to the basket nonpolar interior, the carboxylic groups become situated at the outer side in the polar water solvent (Figure 1 B).

Furthermore, we examined the solid-state structures of eighteen phthalimide derivatives of type Pht–CHR–CO_2H by using the Cambridge structural database (CSD, Figure 1 C). Importantly, there is a conformational bias about the χ_1 torsion with a disposition toward $\chi_1 = 11.1 \pm 7.9^\circ$ (mean $\pm$ standard deviation). Indeed, our computational studies concurred a preference of the C–H bond to nearly eclipse the phthalimide ring due to a) the minimization of the unfavorable van der Waals type of strain between the juxtaposed C=O and CO_2^-/R groups[16]; and b) the maximization of *n*-to-σ* hyperconjugation, whereby C–C bonds act as an electron acceptor, and the lone pair on the phthalimide nitrogen acts as an electron donor (see the Supporting Information). Importantly, the more sizeable R groups in compounds **12** and **14** (Figure 1 A) become almost perpendicular with respect to the imide unit (see the Supporting Information). To summarize, the amino acid side chains of $[\mathbf{1}\text{–}\mathbf{7}]^{3-}$ in water point to the basket inner side, with the C–H bond almost eclipsing the phthalimide group, to face the incoming guest molecule (Figure 1 B).

A fifty-fold dilution of 5.0 mM solution of baskets $[\mathbf{1}]^{3-}$, $[\mathbf{2}]^{3-}$, $[\mathbf{4}]^{3-}$, and $[\mathbf{7}]^{3-}$ in water (pH 7.0 ± 0.1) led to a small decrease in the linewidth of their well-resolved ^{1}H NMR proton resonances (Figures S6–S9 in the Supporting Information). Likewise, a dilution of 5.0 mM aqueous solution of corresponding model compounds $[\mathbf{9}]^{1-}$, $[\mathbf{10}]^{1-}$, $[\mathbf{12}]^{1-}$, and $[\mathbf{15}]^{1-}$ caused a negligible perturbation of their proton resonances (Figures S10–S13 in the Supporting Information). To additionally probe the aggregation, we completed pulse-field gradient NMR spectroscopic measurements of the diffusion of baskets (DOESY, Table 1) and model compounds (Table S1 in the Supporting Information).[17] At 298.1 K, the translational diffusion coefficients were comparable for all four baskets (Table 1), with the corresponding hy-

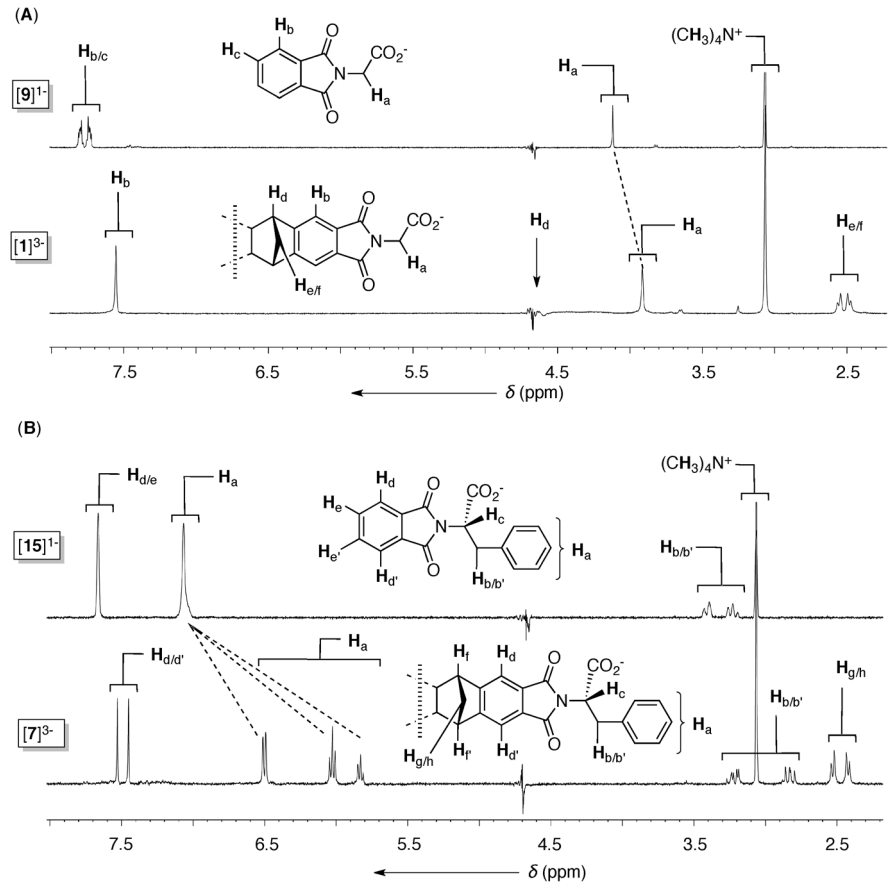

Figure 2. A) ^{1}H NMR spectra (400 MHz, 300.1 K) of basket $[\mathbf{1}]^{3-}$ and model compound $[\mathbf{9}]^{1-}$ (1.0 mM) in aqueous phosphate buffer at pH 7.0 ± 0.1. B) ^{1}H NMR spectra (400 MHz, 300.1 K) of basket $[\mathbf{7}]^{3-}$ and model compound $[\mathbf{15}]^{1-}$ (1.0 mM) in aqueous phosphate buffer (10.0 mM) at pH 7.0 ± 0.1; ^{1}H NMR signals at approximately 4.7 ppm are missing because of the suppression of the water's resonance.

drodynamic radii consistent with the preponderance of monomeric species. No evidence of aggregation was observed for model compounds $[\mathbf{9}]^{1-}$, $[\mathbf{10}]^{1-}$, $[\mathbf{12}]^{1-}$, and $[\mathbf{15}]^{1-}$ (Table S1 in the Supporting Information), in which the self-diffusion coefficients ($D = 6.1–7.6 \times 10^{-10}$ m^2 s^{-1}) suggested the abundance of monomeric species ($r_H = 3.2–3.7$ Å).

An incremental addition of DMMP to $[\mathbf{1}]^{3-}$ in water caused a perturbation of the magnetic environment of proton nuclei in both host and guest, as was monitored by ^{1}H NMR spectroscopy (Figure 3A). In particular, the process of complexation was accompanied with a greater shielding of the guest P–CH_3 ($\Delta\delta = 0.40$ ppm) than P–OCH_3 ($\Delta\delta = 0.16$ ppm) resonances to indicate the insertion of P–CH_3 group inside the cup-shaped scaffold of $[\mathbf{1}]^{3-}$ (Figure 3C).[15] Because the method of continuous variation was in line with 1:1 binding stoichiometry (Figure S14 in the Supporting Information),[18] we subjected the ^{1}H NMR titration data to nonlinear least-square analysis by using a model describing 1:1 complexation occurring at a fast rate on the NMR time scale (Figure 3B).[19] The computed binding isotherm (298.1 K) fits well to the experimental data ($R^2 = 0.997$) and with an association constant of $K_a = 465 \pm 10$ M^{-1} (Figure 3). The formation of 1:1 complex was additionally supported with the results of DOSY NMR measurements: the translational diffusion coefficients of $[\mathbf{1}\subset$DMMP$]^{3-}$ and free $[\mathbf{1}]^{3-}$ host are comparable and in line with their similar size in solution (Table 1).

The interaction of DMPP with basket **1** was additionally examined with molecular dynamics and molecular docking computational protocols (see the Supporting Information). In brief, the simulations confirmed that the [**1**⊂DMPP] complex was dominated by the P–CH_3 group of the guest populating the cavity of **1** (Figure 3C). The methyl group is positioned above the basal aromatic ring, in complete support of the experimental findings.

We subsequently completed the titration of DMMP as a guest to monomeric hosts $[\mathbf{2}–\mathbf{7}]^{3-}$, each carrying increasingly larger amino acids at the rim (Figure 1B, see also Figures S15–S20 in the Supporting Information). Interestingly, the association constants (K_a) varied across the series of hosts: $[\mathbf{1}]^{3-}$ had the largest K_a, whereas $[\mathbf{6}]^{3-}$ had the lowest propensity for entrapping DMMP (Figure 4B). Interestingly, basket $[\mathbf{7}]^{3-}$ showed no measurable affinity toward complexation of DMMP (Figure S20 in the Supporting Information), due to perhaps a high propensity of its benzene moiety for occupying the host's inner space. Because the cup-shaped cavity is retained in all baskets, we presumed that the hydrophobic chains at the rim must be affecting the binding by steric interactions (Figure 4A). To quantify the steric effects,[20] however, one could use various steric parameters of which the Charton's v constants (derived from Taft's E_s values) ascribe a single number to the substituent of interest, thereby approximated as a sphere.[21] Correspondingly, the linear free-energy relationship (LFER) of $\log K_a$ as a function of v was found to be rather inconsistent ($R^2 = 0.63$, Figure S21 in the Supporting Information), suggesting that the shape of amino acid substituents in $[\mathbf{1}–\mathbf{6}]^{3-}$ cannot be treated as spherical.[20] To account for the results, we reasoned that a restricted rotational preference of the hydrophobic groups necessitate a consideration of their multifaceted nature. Indeed, Verloop and co-workers developed a computational program (Sterimol)[22] for characterizing the dimension of functional groups by using three independent parameters: B_1 corresponds to the minimal width, B_5 to the maximal width, and L to the length of the substituent of interest.[23] In particular, minimal width B_1 is a measure of the steric bulk at the first carbon atom of the substituent (Figure 4B) such that the branching at this position affects its value. Notably,

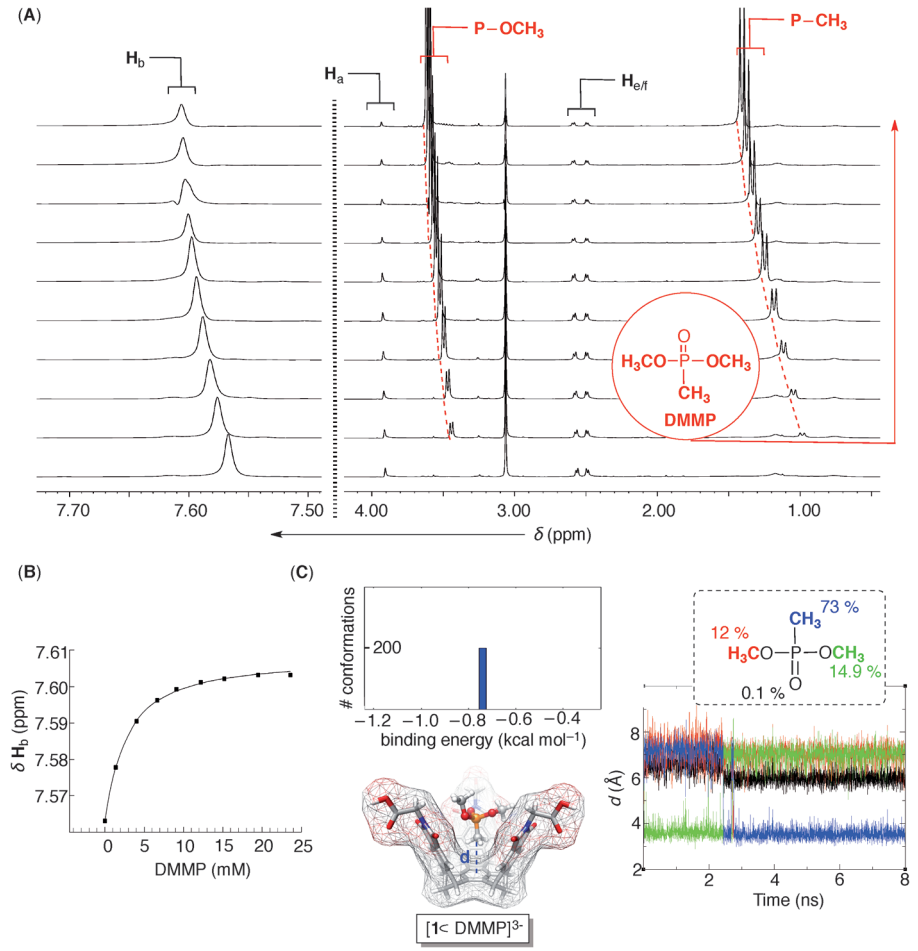

Figure 3. A) Selected ^{1}H NMR spectra (600 MHz, 298.1 K) of basket $[\mathbf{1}]^{3-}$ (1.0 mM), in aqueous phosphate buffer (10.0 mM) at pH 7.0 ± 0.1, obtained upon an incremental addition of DMMP. B) Nonlinear least-square analysis of the binding data (1:1 binding stoichiometry) gave the association constant $K_a = 465 \pm 10\ M^{-1}$ ($R^2 = 0.999$, SigmaPlot) for the formation of $[\mathbf{1}\subset DMMP]^{3-}$. C) Clustering histogram from molecular docking of DMMP into basket of type **1** (top left). Molecular-dynamics results for a subsequent trajectory of the dominant binding mode as a function of time (bottom right), in which the different distances (*d*) between moieties of the DMMP were monitored relative to the centroid of the basal aromatic ring of the basket, leading to a percentage distribution (top right). Energy-minimized structure of $[\mathbf{1}\subset DMMP]^{3-}$ complex (MMFFs, Spartan).

the LFER plot of $\log K_a$ as a function of B_1 showed a more reasonable correlation ($R^2 = 0.90$, Figure 4C) to denote that the proximal steric bulk is important in the recognition. That is to say, the greater the degree of branching at the receptor's rim, the lower the binding affinity of the host towards the DMMP guest. It follows that the branching at the remote carbon does not considerably perturb the encapsulation of organophosphonates, which is useful for guiding the design of more effective hosts in the future.

To probe the validity of the LFER in Figure 4C, we prepared four additional baskets **16**–**19**, each carrying two types of amino acids at the rim (Figure 5A). Importantly, the translational diffusion of $[\mathbf{16}]^{3-}$–$[\mathbf{19}]^{3-}$ ($D = 3.3$–$3.8 \times 10^{-10}\ m^2 s^{-1}$, Table S2 in the Supporting Information) suggested that these compounds stayed monomeric in aqueous solvent at pH 7.0 ± 0.1. The baskets were found to trap DMMP although the stability of $[\mathbf{16}$–$\mathbf{19}\subset DMMP]^{3-}$ complexes (K_a) appeared to be much lower than expected from the established correlation of $\log K_a$ versus ΣB_1 (Figure 4C, see also Figures S22–S25 in the Supporting Information).

To account for the result, we compared ^{1}H NMR spectra of baskets $[\mathbf{4}]^{3-}$, $[\mathbf{16}]^{3-}$, and $[\mathbf{17}]^{3-}$ containing a variable number of valines (3, 2, and 1) at the rim, as well as the valine model compound $[\mathbf{12}]^{1-}$ (Figure 5B). Thus, ^{1}H NMR spectra of $[\mathbf{12}]^{1-}$ and $[\mathbf{4}]^{3-}$ revealed resonances at $\delta =$ 0.3–1.0 ppm corresponding to two diastereotopic methyl groups of which one is more shielded than another (Figure 5B). Perhaps, this is in line with the conformational bias, whereby only one methyl is juxtaposed to the phthalimide ring, with the rotamer III dominating the equilibrium (Figure 5C). In fact, the solid-state structure of **12**[24] shows the existence of this particular conformer (Figure 5C). ^{1}H NMR spectrum of $[\mathbf{16}]^{3-}$, with two glycines and one valine at the rim, revealed an additional upfield shift of one methyl group ($\delta = -0.19$ ppm), whereas another stayed unperturbed (Figure 5B). Because this particular basket has a single hydrophobic amino acid, we deduce that the rotamer II is now dominating the equilibrium, so that both methyl groups populate its hydrophobic inner space in polar water solvent (Figure 5C). In consequence of the conformational transition within $[\mathbf{16}]^{3-}$, the protons of one methyl group became more magnetically shielded (Figure 5C); note that comparable conformational changes were also taking place with other C_1 symmetric baskets **18**–**19** (Figure S26 in the Supporting Information). Because the Verloop's steric parameters were derived for groups in their most stable conformation,[25] the change in the geometry of amino acids within **16**–**19** are not accounted for with the reported B_1 values to, in part, contribute to the observed trend (Figure 4C). Indeed, Verloop and co-workers envisioned that conformational dynamics could be problematic for completing quantitative correlations and in some cases derived another set of parameters.[25] Furthermore, reducing the symmetry of hosts, from C_3 to C_1, could also affect the binding, because less symmetric $[\mathbf{16}$–$\mathbf{19}]^{3-}$ give diastereomeric complexes with DMMP guest adopting different orientations in their cavity.[26]

In conclusion, baskets with amino acids at the rim trap DMMP as an OP guest, akin to sarin in size, in water and near

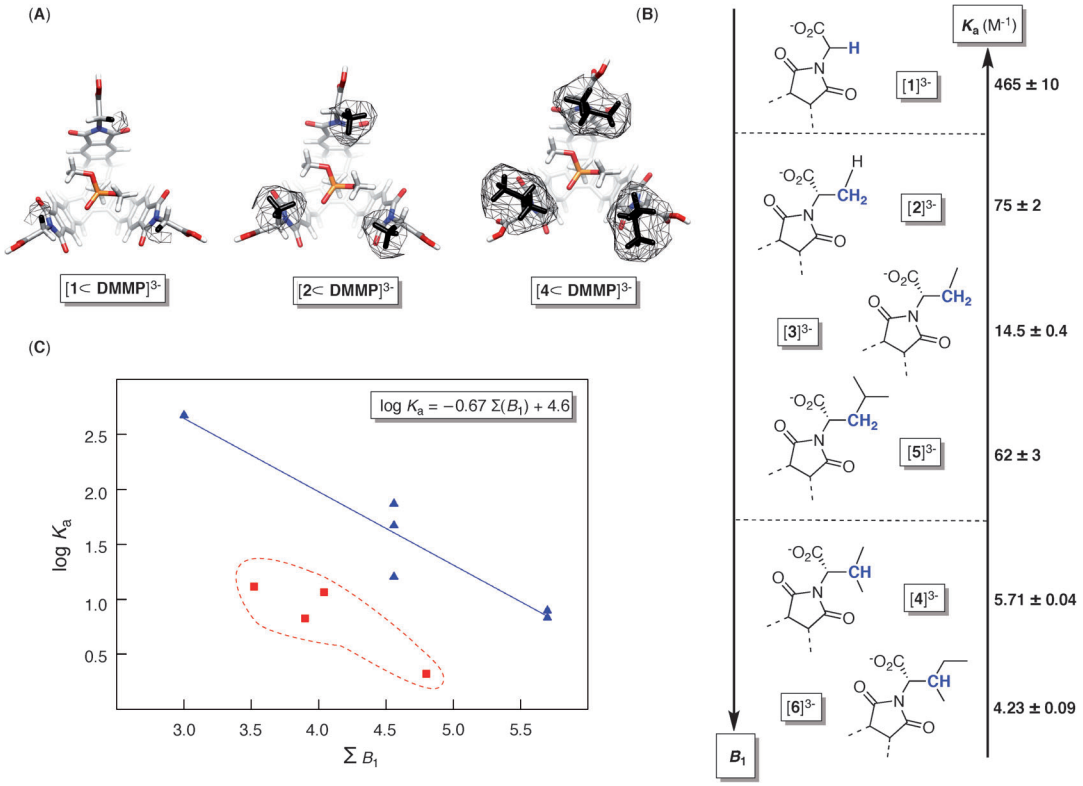

Figure 4. A) Top view of energy-minimized complexes [**1**⊂DMMP]$^{3-}$, [**2**⊂DMMP]$^{3-}$, and [**4**⊂DMMP]$^{3-}$ (MMFFs, Spartan), showing increasingly larger alkyl groups at the basket rim. B) The degree of branching at the first carbon (blue) of the substituent (B_1) is somewhat related to the stability of the complex (K_a from one measurement). C) The linear free-energy relationship (LFER) of log K_a (the arithmetic mean of two measurements), corresponding to the formation of [**1**–**6**⊂DMMP]$^{3-}$ complexes, versus B_1 steric parameters (blue, $R^2 = 0.90$). The binding affinity (log K_a) of C_1 symmetric baskets [**16**]$^{3-}$–[**19**]$^{3-}$ (see Figure 5 for structures) toward DMMP (red) does not obey the established LFER.

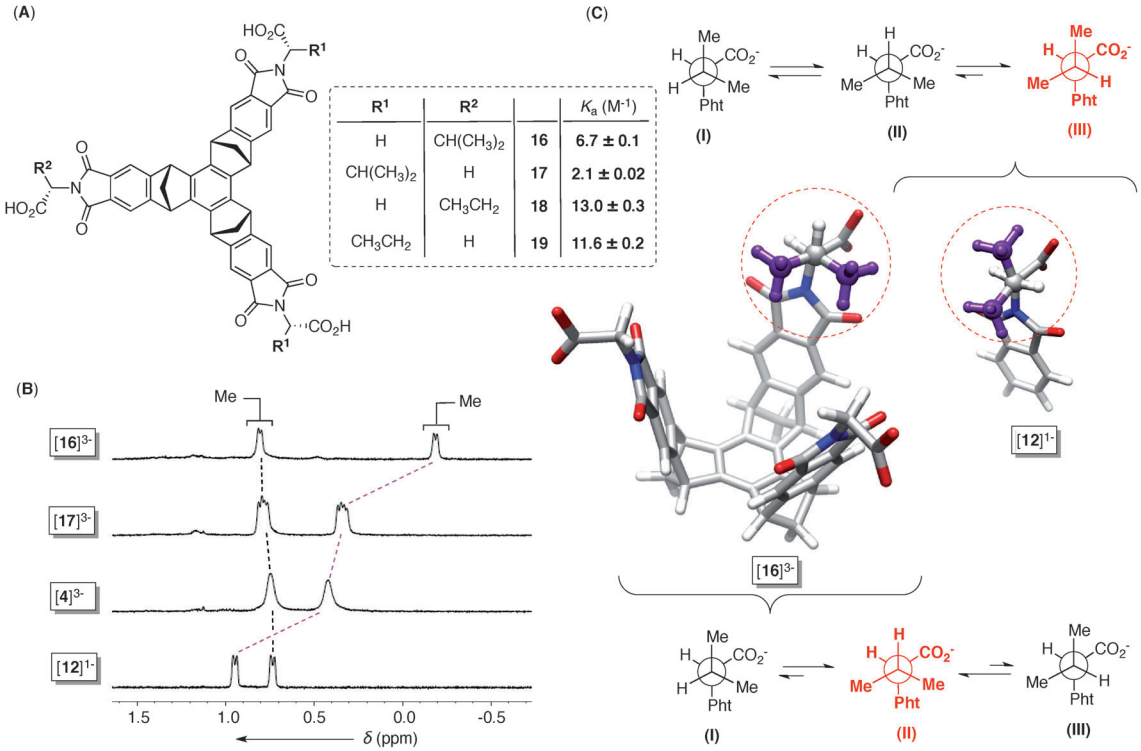

Figure 5. A) Chemical structures of baskets **16**–**19**, each containing two different amino acids; K_a pertaining the entrapment of DMMP with **16**–**19** is described in Figures S22–S25 in the Supporting Information. B) Segments of ^{1}H NMR spectra (400 MHz, 298.1 K) of valine-containing model [**12**]$^{1-}$ and baskets [**4**]$^{3-}$, [**17**]$^{3-}$, and [**16**]$^{3-}$ (1.0 mM in phosphate buffer at pH 7.0 ± 0.1) showing the resonances corresponding to diastereotopic methyl groups. C) Major conformational isomers of basket [**16**]$^{3-}$ and model [**12**]$^{1-}$ (MMFFs, Spartan).

physiological pH. The binding is quantifiable with steric interactions at the rim playing the critical role in the recognition. The results are important for functionalization of baskets toward creating effective artificial scavengers of OP nerve agents and supramolecular degradation catalysts.

Acknowledgements

This work was financially supported with funds obtained from the Department of Defense, Defense Threat Reduction Agency (HDTRA1-11-1-0042). The content of the information does not necessarily reflect the position or the policy of the federal government, and no official endorsement should be inferred. Computational support from the Ohio Supercomputer Center is gratefully acknowledged.

Keywords: host–guest systems · linear free-energy relationship · molecular encapsulation · molecular recognition · nerve agents

[1] a) A. E. Hargrove, S. Nieto, T. Zhang, J. L. Sessler, E. V. Anslyn, *Chem. Rev.* **2011**, *111*, 6603 – 6782; b) C. Tudisco, P. Betti, A. Motta, R. Pinalli, L. Bombaci, E. Dalcanale, G. G. Condorelli, *Langmuir* **2012**, *28*, 1782 – 1789; c) M. R. Sambrook, J. R. Hiscock, A. Cook, A. C. Green, I. Holden, J. C. Vincent, P. A. Gale, *Chem. Commun.* **2012**, *48*, 5605 – 5607; d) C. Montoro, F. Linares, E. Quartapelle Procopio, I. Senkovska, S. Kaskel, S. Galli, N. Masciocchi, E. Barea, J. A. R. Navarro, *J. Am. Chem. Soc.* **2011**, *133*, 11888 – 11891; e) C. Van Hooidonk, J. C. A. E. Breebaart-Hansen, *Recl. Trav. Chim. Pays-Bas* **1970**, *89*, 289 – 299; f) B. Desire, S. Saint-Andre, *Fundam. Appl. Toxicol.* **1986**, *7*, 646 – 657; g) R. Le Provost, T. Wille, L. Louise, N. Masurier, S. Mueller, G. Reiter, P.-Y. Renard, O. Lafont, F. Worek, F. Estour, *Org. Biomol. Chem.* **2011**, *9*, 3026 – 3032; h) M. Zengerle, F. Brandhuber, C. Schneider, F. Worek, G. Reiter, S. Kubik, *Beilstein J. Org. Chem.* **2011**, *7*, 1543 – 1554; i) N. A. Esipenko, P. Koutnik, T. Minami, L. Mosca, V. M. Lynch, G. V. Zyryanov, P. Anzenbacher Jr., *Chem. Sci.* **2013**, *4*, 3617 – 3623.

[2] K. Kim, O. G. Tsay, D. A. Atwood, D. G. Churchill, *Chem. Rev.* **2011**, *111*, 5345 – 5403.

[3] D. Elie, *Nat. Med.* **2013**, *19*, 1194 – 1195.

[4] a) S. S. Talmage, A. P. Watson, V. Hauschild, N. B. Munro, J. King, *Curr. Org. Chem.* **2007**, *11*, 285 – 298; b) Y. C. Yang, J. A. Baker, J. R. Ward, *Chem. Rev.* **1992**, *92*, 1729 – 1743.

[5] S. Chauhan, S. Chauhan, R. D'Cruz, S. Faruqi, K. K. Singh, S. Varma, M. Singh, V. Karthik, *Environ. Toxicol. Pharmacol.* **2008**, *26*, 113 – 122.

[6] a) Z. Radic, T. Dale, Z. Kovarik, S. Berend, E. Garcia, L. Zhang, G. Amitai, C. Green, B. Radic, B. M. Duggan, D. Ajami, J. Rebek, P. Taylor, *Biochem. J.* **2013**, *450*, 231 – 242; b) M. Pohanka, *Anal. Lett.* **2013**, *46*, 1849 – 1868; c) H. Mumford, C. J. Docx, M. E. Price, A. C. Green, J. E. H. Tattersall, S. J. Armstrong, *Chem.-Biol. Interact.* **2013**, *203*, 160 – 166.

[7] a) T. T. Sanan, S. Muthukrishnan, J. M. Beck, P. Tao, C. J. Hayes, T. C. Otto, D. M. Cerasoli, D. E. Lenz, C. M. Hadad, *J. Phys. Org. Chem.* **2010**, *23*, 357 – 369; b) D. T. Yeung, D. E. Lenz, D. M. Cerasoli, *Proteins Cell Regul.* **2008**, *6*, 151 – 170.

[8] a) D. J. Cram, *Nature* **1992**, *356*, 29 – 36; b) D. J. Cram, *Science* **1983**, *219*, 1177 – 1183.

[9] F. Hof, S. L. Craig, C. Nuckolls, J. Rebek, Jr., *Angew. Chem.* **2002**, *114*, 1556 – 1578; *Angew. Chem. Int. Ed.* **2002**, *41*, 1488 – 1508.

[10] S. Rieth, K. Hermann, B.-Y. Wang, J. D. Badjic, *Chem. Soc. Rev.* **2011**, *40*, 1609 – 1622.

[11] J. D. Badjic, S. Stojanovic, Y. Ruan, *Adv. Phys. Org. Chem.* **2011**, *45*, 1 – 37.

[12] D. Ajami, J. Rebek, *Org. Biomol. Chem.* **2013**, *11*, 3936 – 3942.

[13] B. M. Smith, *Chem. Soc. Rev.* **2008**, *37*, 470 – 478.

[14] S. Chen, Y. Ruan, J. D. Brown, J. Gallucci, V. Maslak, C. M. Hadad, J. D. Badjic, *J. Am. Chem. Soc.* **2013**, *135*, 14964 – 14967.

[15] Y. Ruan, H. A. Taha, R. J. Yoder, V. Maslak, C. M. Hadad, J. D. Badjic, *J. Phys. Chem. B* **2013**, *117*, 3240 – 3249.

[16] a) B.-Y. Wang, S. Stojanovic, D. A. Turner, T. L. Young, C. M. Hadad, J. D. Badjic, *Chem. Eur. J.* **2013**, *19*, 4767 – 4775; b) S. Stojanovic, D. A. Turner, A. I. Share, A. H. Flood, C. M. Hadad, J. D. Badjic, *Chem. Commun.* **2012**, *48*, 4429 – 4431; c) S. Stojanovic, D. A. Turner, C. M. Hadad, J. D. Badjic, *Chem. Sci.* **2011**, *2*, 752 – 759.

[17] Y. Cohen, L. Avram, L. Frish, *Angew. Chem.* **2005**, *117*, 524 – 560; *Angew. Chem. Int. Ed.* **2005**, *44*, 520 – 554.

[18] K. Hirose, *Anal. Methods Supramol. Chem.* **2007**, 17 – 54.

[19] *Frontiers in Supramolecular Organic Chemistry and Photochemistry* (Eds.: H. J. Schneider, H. Duerr), Wiley, New York, **1991**.

[20] K. C. Harper, E. N. Bess, M. S. Sigman, *Nat. Chem.* **2012**, *4*, 366 – 374.

[21] a) M. Charton, *J. Org. Chem.* **1976**, *41*, 2217 – 2220; b) M. Charton, *J. Am. Chem. Soc.* **1975**, *97*, 1552 – 1556; c) M. Charton, *J. Am. Chem. Soc.* **1975**, *97*, 3691 – 3693.

[22] a) A. Verloop, *Pestic. Chem. Hum. Welfare Environ., Proc. Int. Congr. Pestic. Chem. 5th* **1983**, *1*, 339 – 344; b) *Topics in Current Chemistry, Vol. 114: Steric Effects in Drug Design* (Eds.: M. Charton, I. Motoc), Springer, Berlin – Heidelberg, **1983**.

[23] P. Krogsgaard-Larsen, T. Liljefors, U. Madsen, *Textbook of Drug Design and Discovery*, 3rd ed., Taylor & Francis, London, **2002**.

[24] A. R. Raza, A. Saddiqa, M. N. Tahir, S. Saddiq, *Acta Crystallogr. Sect. A Acta Crystallogr. Sect. E Struct. Rep. Online* **2011**, *67*, o2435.

[25] *Medicinal Chemistry, Vol. 11: Drug Design, Vol. 7*: (Ed.: E. J. Ariens), Medicinal Chemistry Acadmeic Press, New York, **1976**.

[26] a) C. Moberg, *Angew. Chem.* **1998**, *110*, 260 – 281; *Angew. Chem. Int. Ed.* **1998**, *37*, 248 – 268; b) C. Moberg, *Angew. Chem.* **2006**, *118*, 4838 – 4840; *Angew. Chem. Int. Ed.* **2006**, *45*, 4721 – 4723.

Received: December 5, 2013
Published online on March 11, 2014

